Earth and Planetary Science Letters 369–370 (2013) 59–70

Contents lists available at SciVerse ScienceDirect

Earth and Planetary Science Letters

journal homepage: www.elsevier.com/locate/epsl

Sill to surface: Linking young off-axis volcanism with subsurface melt at the overlapping spreading center at 9°03′N East Pacific Rise

Christopher L. Waters [a,b,*], Kenneth W.W. Sims [a,b], Emily M. Klein [c], Scott M. White [d], Mark K. Reagan [e], Guillaume Girard [e]

[a] Department of Geology and Geophysics, University of Wyoming, Laramie, WY 82072, USA
[b] Department of Geology and Geophysics, Woods Hole Oceanographic Institution, Woods Hole, MA 02543, USA
[c] Division of Earth and Ocean Sciences, Nicholas School of the Environment, Duke University, Durham, NC 27708, USA
[d] Department of Earth and Ocean Sciences, University of South Carolina, Columbia, SC 29208, USA
[e] Department of Geoscience, University of Iowa, Iowa City, IA 52242, USA

ARTICLE INFO

Article history:
Received 10 April 2012
Received in revised form
26 February 2013
Accepted 5 March 2013
Editor: T. Elliott
Available online 20 April 2013

Keywords:
U-series
East Pacific Rise
mid-ocean ridge basalt
off-axis
submarine volcanism

ABSTRACT

No young, off-axis, mid-ocean ridge lavas have yet been directly linked to underlying off-axis melt bodies. In this study, we present new measurements of ^{238}U–^{230}Th–^{226}Ra–^{210}Pb isotope compositions for a suite of lavas from the overlapping spreading center (OSC) at 9°03′N on the East Pacific Rise (EPR). These lavas span a large range of compositions, from basalt to dacite, and include both axial and off-axis samples recovered from a prominent, axis-parallel pillow ridge and a flat-topped seamount that overlie the westernmost extent of a 4-km-wide melt lens (Kent et al., 2000). We report ^{210}Pb excesses in axial basalts and basaltic andesites, which we suggest results from gas-magma fractionation of ^{222}Rn from ^{226}Ra beneath dacite magmas. In addition, our U-series ages agree with visual observations, indicating that while most recent volcanic activity occurs at the spreading axis, active volcanism also occurs away from the axis. Specifically, the off-axis pillow ridge and seamount samples overlying the off-axis subsurface melt body have eruption ages of less than 8 ka, and likely as young as 1 ka, despite being located on crust that has a spreading age of ~75 ka. The young ages of these lavas, combined with existing geological, geochemical and geophysical constraints, provide evidence for a genetic link between the pillow ridge and seamount lavas and the seismically imaged, underlying off-axis melt lens. This link demonstrates that off-axis volcanism does not necessarily come from a sub-axial magma body and can be sourced directly from off-axis magma bodies.

1. Introduction

The relationship between axial volcanism and the underlying axial magma chamber at fast-spreading mid-ocean ridges has long been established (e.g., Sinton and Detrick, 1992), but there has been no definitive evidence linking off-axis volcanism with off-axis magma bodies. Off-axis eruptions are known to occur along the East Pacific Rise (EPR), including large off-axis lava fields, small volcanic cones, and seamounts (Batiza and Vanko, 1984; Hall and Sinton, 1996; Geshi et al., 2007; White et al., 2002; Sims et al., 2003). However, the origin of these lavas with regards to their crustal magma source remains speculative largely because of the lack of (1) comprehensive seismic imaging of crust underlying off-axis lava fields and (2) absolute ages of off-axis lavas.

The overlapping spreading center (OSC) at 9°03′N EPR presents an ideal opportunity for studying the relationships between volcanism and magmatism because the subsurface melt distribution and seafloor morphology have recently been well-characterized in a number of geophysical and geological studies (e.g., Bazin et al., 2003; Combier et al., 2008; Dunn et al., 2001; Kent et al., 2000; White et al., 2009). Using ^{238}U–^{230}Th–^{226}Ra–^{210}Pb age dating, we identify young, axis-parallel volcanism (< 8 ka) up to ~4 km off-axis that directly overlies the western extent of a seismically imaged melt sill (Kent et al., 2000). The young ages for these off-axis lavas, combined with other geologic, petrologic, and geophysical constraints, provide, for the first time, substantive evidence for a genetic link between young off-axis volcanism and subsurface melt.

2. Geological background and sample descriptions

The East Pacific Rise from 8–10°N is a fast-spreading ridge segment (half-spreading rate of 5.5 cm/yr) bounded to the north by the Clipperton Fracture Zone and to the south by the Siqueiros Fracture Zone (Fig. 1). The OSC at 9°03′N EPR consists of two north–south trending spreading axes that overlap by ~27 km and are offset to the right by ~8 km. Geophysical studies document

* Correspondence to: University of California San Diego, Geosciences Research Division, Scripps Institution of Oceanography, 9500 Gilman Drive, La Jolla, CA 92093-0244, USA. Tel.: +1 858 534 4716.
E-mail address: clwaters@ucsd.edu (C.L. Waters).

0012-821X/$ - see front matter © 2013 Elsevier B.V. All rights reserved.
http://dx.doi.org/10.1016/j.epsl.2013.03.006

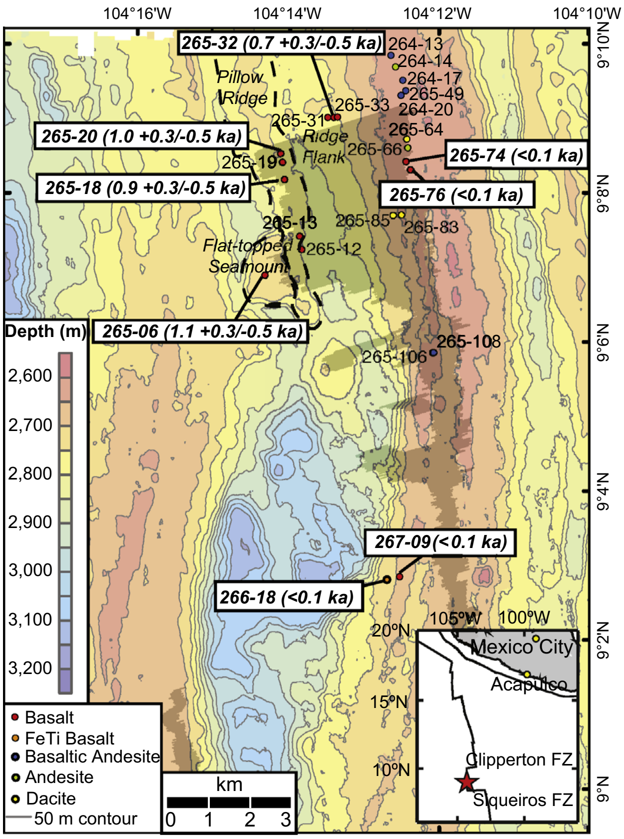

Fig. 1. Compiled bathymetric map (White et al., 2009) of the study area showing sample locations, rock types, and model ages with uncertainties. Dashed lines encircle the off-axis pillow ridge and flat-topped volcano that overlie the western extent of seismically imaged melt (shown as gray overlay; Kent et al., 2000). The inset map locates the study area.

a low velocity anomaly interpreted as melt in the uppermost mantle extending across the OSC, with the lowest velocities centered beneath the eastern limb (Dunn et al., 2000; Toomey et al., 2007), melt accumulation in the overlying crust (Singh et al., 2006), and a mid-crustal mush zone at the northern end of the overlap basin at ~9°08′N (Bazin et al., 2003; Crawford and Webb, 2002). In addition, a 3-D seismic reflection study reveals a ~4 km wide, upper-crustal melt sill beneath the eastern limb that extends westward into the northern portion of the overlap basin (Kent et al., 2000). The sill reflectors deepen to the west of the east limb axis, suggesting melt may be delivered from an off-axis asthenospheric source to the deeper, off-axis part of this melt sill. The melt sill imaged by Kent et al. (2000) is shown as a shaded area in Fig. 1 for reference. However, this melt "sill" is not clearly a continuous melt-rich region, but it is instead complex in 3-D geometry and distribution and may include a network of isolated melt-rich regions away from the melt accumulation underlying the axial graben (cf., Fig. 3d of Singh et al., 2006).

One of the objectives of the AT15-17 cruise to the OSC at 9°03′N EPR was to use the ROV *Jason II* to sample lavas along and across the wide melt lens (Fig. 1; Klein et al., 2007). We selected 22 of these samples for ^{238}U–^{230}Th–^{226}Ra–^{210}Pb isotopic age dating. These samples span a range of tholeiitic volcanic rock compositions, including ferrobasalt, basaltic andesite (or basaltic icelandite), andesite (or icelandite; cf., Carmichael, 1964), and dacite (Wanless et al., 2010, 2011, 2012); and, tectonic settings including the axial graben, the ridge flank, and the large, axis-parallel pillow ridge and flat-topped seamount that overlie the westernmost extent of the wide melt lens (Fig. 1). Sample locations are shown in Fig. 1, sample site photos are shown in Fig. 2, and sample descriptions and compositional variations are given in Supplemental Table 1. Sample major and trace element compositions have been published elsewhere (Wanless et al., 2010, 2011, 2012).

3. Dating lavas with U–Th–Ra disequilibria

The half-lives of U-series nuclides ^{210}Pb (22.6 yr), ^{226}Ra (1.6 ka) and ^{230}Th (75 ka) make them ideally suited for studying recent magmatic and volcanic processes. U-series parent/daughter nuclide pairs can fractionate during partial melting and crystallization, creating radioactive disequilibria. Radioactive decay during melt transport, crustal residence, and post-eruption aging return these nuclide pairs to a steady-state condition called "secular equilibrium," in which the activities of nuclides are equal and the activity ratios (e.g., ($^{210}Pb/^{226}Ra$), ($^{226}Ra/^{230}Th$), ($^{230}Th/^{238}U$)) are unity. Secular equilibrium is reached in roughly five half-lives following the fractionation of parent/daughter nuclides. Therefore, the presence of disequilibrium in a lava, for example ($^{210}Pb/^{226}Ra$)$\neq$1$\pm$0.05 (2SE), ($^{226}Ra/^{230}Th$)$\neq$1$\pm$0.05 (2SE), or ($^{230}Th/^{238}U$)$\neq$1$\pm$0.01 (2SE), limits the eruption age to <100 yr, <8 ka, or <375 ka, respectively.

U-series model age dating of young MORB at the EPR is well established (Goldstein et al., 1994; Rubin and MacDougall, 1990; Sims et al., 2003; Waters et al., 2011). U-series model ages for off-axis MORB have been calculated by inferring initial activities from the youngest axial basalts and comparing these activities with the values measured in off-axis samples of unknown age. Robust application of U-series model ages requires that the young, axial lavas (of known age) and the off-axis lavas of unknown age (to be dated) derive from chemically similar mantle sources and were generated by similar petrogenetic and magmatic processes (Sims et al., 2003). While early models used measurements from one or two axial lavas to calculate the ages of older lavas (e.g., Goldstein et al., 1994), at 9°17′–9°54′N EPR there are now enough young axial lavas of known age that form coherent trends of ^{238}U–^{230}Th–^{226}Ra disequilibria (Sims et al., 2002, 2003) such that this technique is ever more robust (Sims et al., 2003; Waters et al., 2011).

4. Results

4.1. $^{87}Sr/^{86}Sr$ and $^{143}Nd/^{144}Nd$ Isotope compositions

Source lithology can significantly influence the magnitude of ^{238}U–^{230}Th–^{226}Ra disequilibria (e.g., Elkins et al., 2011; Lundstrom et al., 1995; Waters et al., 2011). All measured east limb lavas have uniform $^{87}Sr/^{86}Sr$ and $^{143}Nd/^{144}Nd$ isotope compositions (Table 1), within analytical uncertainties, and are consistent with isotopic compositions previously reported for east limb lavas (Wanless et al., 2010) and basalts from 9°17′N–9°54′N EPR (Goss et al., 2010; Sims et al., 2002, 2003; Waters et al., 2011). This isotopic homogeneity indicates that their time-integrated parent/daughter Rb/Sr and Sm/Nd are uniform, suggesting that these lavas either come from a homogeneous mantle source that is similar to the mantle source for lavas from 9°17′–9°54′N EPR, or that any melts derived from compositional heterogeneities are diluted and masked by thorough mixing (cf. Waters et al., 2011).

4.2. U-series disequilibria

For submarine lavas, ($^{234}U/^{238}U$) is a sensitive indicator of alteration because seawater is significantly enriched in ^{234}U relative to ^{238}U (seawater ($^{234}U/^{238}U$)=1.14$\pm$0.03; Thurber, 1962). All but three samples measured have ($^{234}U/^{238}U$)=1.000$\pm$0.5%